## RESEARCH ARTICLE

# High-Gain Circularly Polarized Antenna Array for Full Incident Angle Coverage in RF Energy Harvesting

**MOHAMMED CHERIF DERBAL** AND **MOURAD NEDIL**, (Senior Member, IEEE)

Underground Communications Research Laboratory, Engineering School, University of Quebec at Abitibi-Témiscamingue (UQAT), Val-d'Or, QC J9P 1Y3, Canada

Corresponding author: Mohammed Cherif Derbal (mohammedcherif.derbal@uqat.ca)

**ABSTRACT** In this paper, a high-gain circularly polarized (CP) hexagonal antenna array is proposed for RF energy-harvesting applications. The hexagonal antenna array is intended to operate at the frequency of 5.8 GHz. It is composed of 6 multilayer substrate CP antennas excited by an X-shaped aperture-coupling feed structure. A frequency selective surface (FSS) was added to further improve the gain, resulting in a maximum gain of 12.7 dBi per element. The main advantage of the proposed hexagonal antenna array is the ability to cover 360 degrees in the azimuth plane with a high gain in all directions without the use of any additional circuitry, allowing the effective absorption of ambient RF energy. A prototype was fabricated and measured, and a good agreement with the simulation results is achieved. In addition, a rectifier is used to convert RF energy absorbed by the antenna into DC energy at the frequency of 5.8 GHz. The measured RF-to-DC conversion efficiency of 44.5% and a DC output voltage of 423 mV at −10 dBm are observed. The performance of the rectenna array with one and six rectifiers has been demonstrated. With the use of a DC combiner, the total RF to DC efficiency of the array is 67.75%, with a DC output voltage of 1.115 V from −10 dBm has been recorded. Due to the immunity to misalignment of the CP antenna, the proposed rectenna array is very suitable for wireless power transfer (WPT).

**INDEX TERMS** RF energy harvesting, high gain, antenna array, full angle coverage.

## I. INTRODUCTION

Wireless sensor networks (WSNs) for internet of things (IoT) applications have grown tremendously in recent years, resulting in a need for self-powered devices to avoid the maintenance and replacement of batteries. In fact, ambient RF energy harvesting is a potential technique to fulfill the concern of battery-less devices. The use of wireless communication systems such as Wi-Fi and mobile communications never ceases to increase in everyday activities, and as a result, ambient RF energy is abundant almost everywhere, which makes it a strong technique to power devices [1]. To convert ambient RF energy into DC power, a rectenna (rectifying antenna) is necessary.

The associate editor coordinating the review of this manuscript and approving it for publication was Giorgio Montisci.

However, there are two main drawbacks of ambient RF energy harvesting. The first is the low power density of RF signals available, which causes low RF–DC conversion efficiency [2], [3], [4] in the environment. To overcome this issue, several research works have been reported, suggesting different solutions [5], [6], [7], [8]. In [5], a high gain rectenna of 8.5 dBi for the GSM band has been introduced. Similarly, a rectenna for the Wi-Fi band has been reported in [6]. Antenna arrays have also been introduced to absorb more RF energy given their high gain compared to a single antenna [7], [8].

Second, the random distribution of the available RF energy is the most challenging problem for RF energy harvesting. In fact, the position of the RF transmitter or the orientation of the rectenna varies with time, which means that the ambient RF energy arrives at the antenna from random angles [9]. A few works have been proposed lately to solve this issue.

In [10], a dipole antenna was used given its omnidirectional radiation pattern to allow absorbing RF signals from all directions, but this antenna exhibits a poor gain. To absorb RF energy in a wide incident-angles range, a $4 \times 4$ Butler matrix with hybrid couplers was used for the beam-forming matrix in a hybrid power-combining rectenna array [11]. This approach allows the antenna to receive RF signals from a wide coverage angle of 146 degrees. A cylindrical antenna array composed of 5 vertical antenna arrays is introduced in [9]. Hence a full spatial coverage was obtained using beam-forming networks ($4 \times 4$ Butler matrix) with a maximum gain of 4 dBi. However, the drawbacks are either the poor gain or the complexity of the design by using additional circuitry such as coupler and cross overs in the Butler matrix system.

In this contribution, a high gain and low-profile 6-port CP hexagonal rectenna array is introduced. This array offers full spatial coverage to absorb RF energy at the frequency of 5.8 GHz from the full 360 degrees in the azimuth plane. In addition, a frequency selective surface (FSS) is introduced on each element of the array to reach a maximum gain of 12.7 dBi per element. The rectifier has been also designed to convert the RF energy absorbed from the Wi-Fi band to DC energy. The main advantage of this array is the full spatial coverage and significantly high gain at the same time with the ease of fabrication without using any additional circuitry. Furthermore, the antenna system has 6 ports, which add to the possibility to further enhance the DC voltage or current output by using a DC combiner.

## II. THE HEXAGONAL ANTENNA ARRAY DESIGN

The layout of the suggested microstrip coupled antenna (MCA) is shown in Figure 1. It has been chosen for this work because of its high gain and good radiation efficiency, which makes it highly suitable for RF energy-harvesting application. It is designed to operate at the frequency of 5.8 GHz, and it is composed of three layers. The first layer is a microstrip feed line etched on the bottom side of RT/Duroid 5880 substrate ($\varepsilon r = 2.2$ and 0.787 mm of thickness) and the ground plane with an X-shaped coupling aperture on the other side. This is followed by foam of 3 mm thickness, with a low dielectric constant $\varepsilon r = 1.07$. The patch was etched on RT/Duroid 5880 substrates with a dielectric constant equal to 2.2 and with 0.127 mm of thickness.

The radiation mechanism is accomplished by allowing electromagnetic energy provided by the feed microstrip line to pass through the X-shaped aperture into the patch. It is possible to achieve equal amplitudes and phase quadrature for both orthogonal modes TM100 and TM010 excited in the same resonator by making an appropriate selection of the patch and the X-shaped aperture dimensions. The energy of the produced CP electromagnetic field is emitted into space in the direction of the antenna's broadside radiation pattern.

For the gain enhancement, the FSS was introduced to the antenna system, as illustrated in Figure.1. As shown in Figure 2, the square shape has been chosen as the unit cell structure for bandwidth and stability performances. Hence,
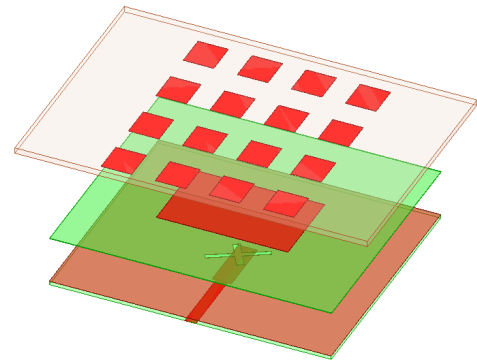


**FIGURE 1.** Layout of the proposed antenna with the FSS layer.

the FSS design is carried out by optimizing and improving the FSS unit size via Floquet port simulation on CST software 2019. Figure 3 shows the S-parameters of the FSS unit cell.
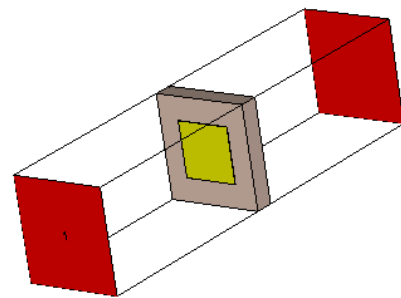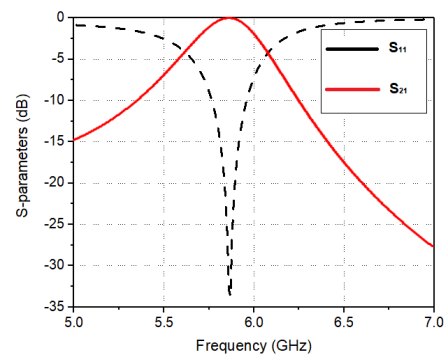


**FIGURE 2.** FSS unit cell.



**FIGURE 3.** S-parameters of the proposed FSS unit cell.

The dimensions of the FSS substrate, the number, and the size of the unit cells were optimized using the CST microwave studio. The unit cells are printed on the bottom side of a 1.27 mm–thick RT/Duroid 5870 superstrates with a dielectric constant of 10.7. The dimensions of the proposed antenna are illustrated in Figure 4 (unit: millimeter).

Figure 5 illustrates the impact of the distance $d$ between the FSS and the antenna on the overall return loss of the proposed structure. This distance is an important factor to achieve good impedance matching of the antenna system as it will directly affect the resonance frequency of the antenna; thus, it has

been carefully optimized. To obtain the desired return loss, numerous parametric sweeps were carried out. The distance *d* was varied to obtain the optimal return loss. It was observed that a good scattering parameter was obtained at 25 mm; on the other hand, for all the other distances, the return loss is not well matched at the frequency 5.8 GHz.
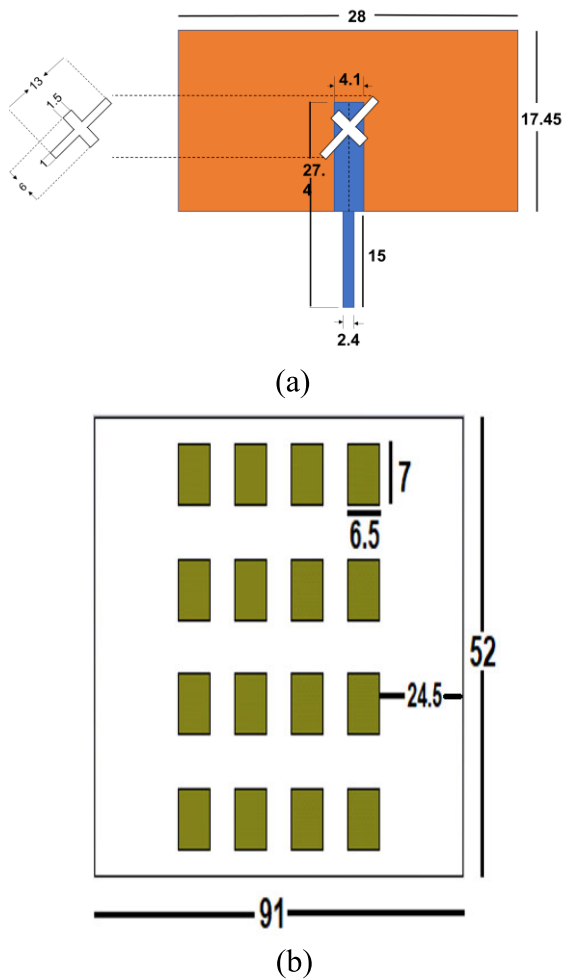


(a)



(b)

**FIGURE 4.** Dimensions of the proposed structure: (a) antenna; (b) FSS.

A prototype of the presented antenna with the FSS layer has been fabricated (Figure 6). The comparison between the measured and simulated reflection coefficients is depicted in Figure 7a.

In this case, it can be observed that the measured results are consistent with the simulated outcomes.

Thus, the antenna operates well at the frequency band of 5.8 GHz with a good impedance matching performance. From Figure 7b, we can observe that the antenna has an axial ratio equal to 1.2 at the frequency 5.8 GHz; hence, the proposed antenna presents CP polarization at this band.

It was necessary to model the surface current distributions on the patch at different phases to verify the production of the RHCP (see Figure 8). The simulation was performed using CST. Figure 7 depicts the simulated surface current
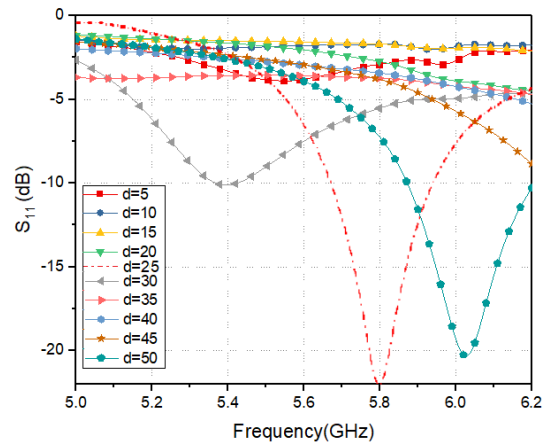


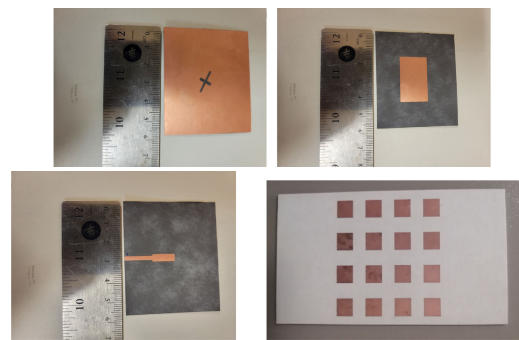**FIGURE 5.** S-parameters of the antenna at various distances *d*.



**FIGURE 6.** Fabricated prototype.

distributions at 0°, 90°, 180°, and 270°. At 0°, the vector sum of the currents points from the upper side to the lower side. The major currents lie in the middle of the patch at 90°, resulting in a vector sum pointing from the right to the left of the patch; this vector sum is orthogonal to that at 0°. It can be observed that the surface current from the antenna rotates in a clockwise direction, thereby generating the RHCP.

The measured and simulated radiation patterns of the antenna with FSS in the H-plane and E-plane at the frequency 5.8 GHz are shown in Figure 9. The results show a directive radiation pattern in both planes and a good correlation between the measured and simulated results.

Because of the FSS layer, the proposed structure has reached a maximum gain of 12.7 dBi, as depicted in Figure 10. The antenna without FSS has a maximum gain of 8 dBi at the frequency 5.8 GHz by adding the FSS superstrate to the antenna; a maximum gain of 12.9 dBi is obtained with a gain enhancement of 4.9 dBi. The maximum measured gain of the antenna with FSS is 12.7 dBi at the frequency 5.8 GHz.

The proposed 6-port hexagonal array has two main objectives: high gain and full coverage without using any additional circuitry. The proposed array is composed of six elements of the previously presented antenna set in a hexagonal configuration. Each antenna was optimized to cover a specific direction with a 3 dB beam width equal to 60 degrees, which
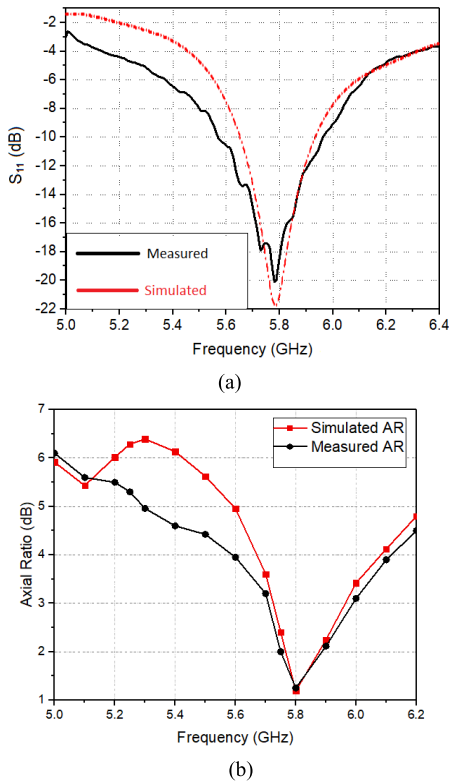
(a)



(b)

**FIGURE 7.** Measured results of the proposed antenna with the FSS layer: (a) S-parameters; (b) axial ratio.
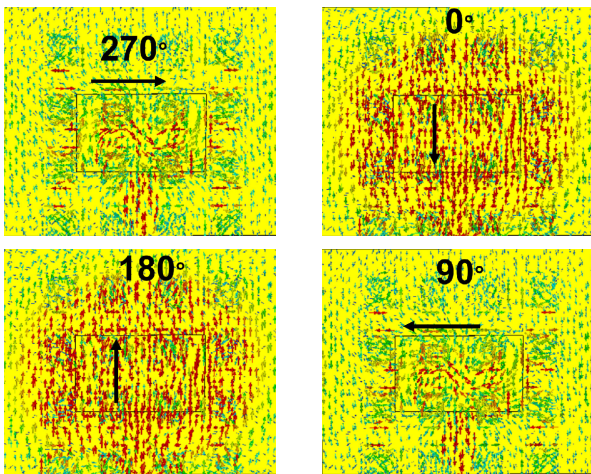


(a)



(b)

**FIGURE 9.** Radiation patterns at the frequency 5.8 GHz: (a) H-plane; (b) E-plane.



**FIGURE 8.** Surface current density at different phases at the center frequency 5.8 GHz.
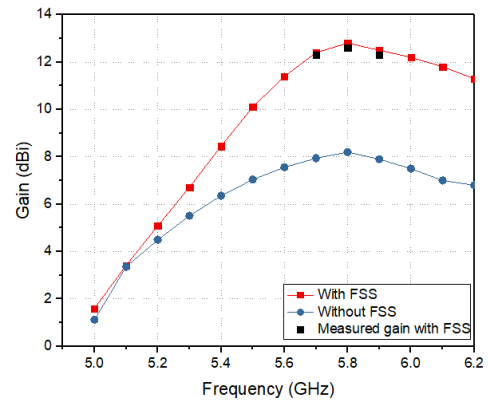


**FIGURE 10.** Gain of the proposed antenna versus frequency.

allows covering all the azimuth plane efficiently. The fabricated hexagonal array is presented in Figure 11.

The measured reflection coefficients of the hexagonal array for ports 1, 2, and 3 are shown in Figure 12. All the ports have a good impedance matching at the frequency band of 5.8 GHz. Given the symmetrical geometry of the antenna array, ports 4, 5, and 6 have almost the same reflection coefficients as ports 1, 2, and 3, respectively.
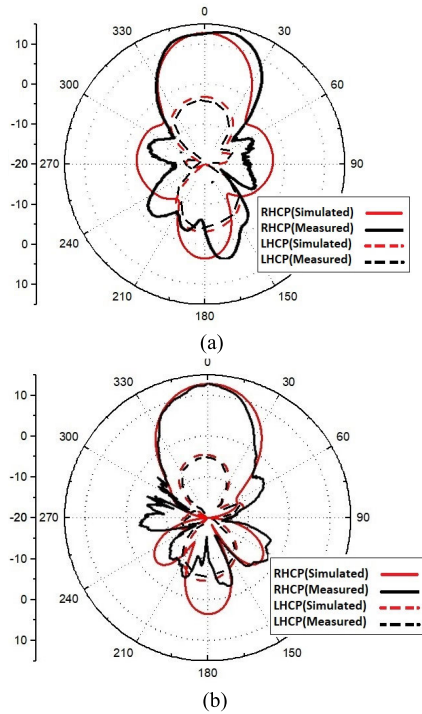
The 3D radiation pattern of the antenna array is shown in Figure 13. When one element of the array is fed, a directional radiation pattern of 12.7 dBi is noticed in Figure 13a.

Figure 13b and 13c illustrates the 3D and polar radiation pattern of the antenna array when all the elements are fed. The array can radiate in all directions in the azimuth plane with a maximum gain of 12.7 dBi on each antenna element, allowing covering the entire azimuth plane with no blind spot, which demonstrates the ability of the proposed array to efficiently absorb RF energy from any direction.

This radiation characteristic of the proposed antenna makes it highly suitable for RF energy-harvesting applications. In addition, a total efficiency of 97.2% of each element in the array is recorded.
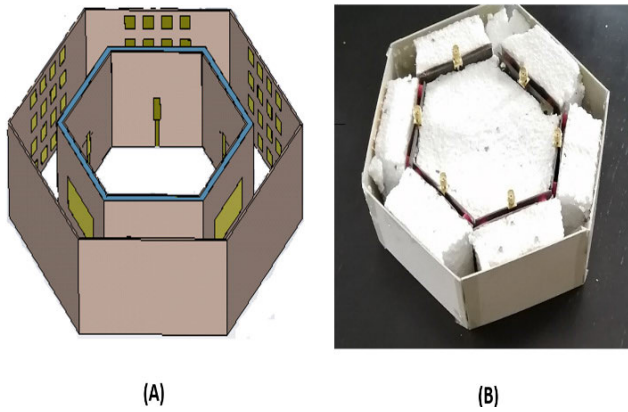
**FIGURE 11.** A 6-port hexagonal array: (a) layout of the hexagonal array; (b) fabricated prototype.
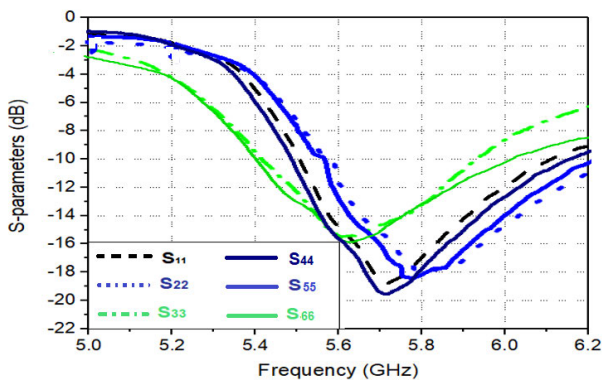


**FIGURE 12.** Measured S-parameters of the hexagonal array.

## III. RECTIFIER DESIGN

The schematic of the designed rectifier is shown in Figure 14. The impedance matching of the rectifier strongly depends on three main factors: the frequency of operations, the input power, and the load $R_L$. These factors should be carefully chosen to be well suitable for the environment in which the rectifier will be used as well as the application.

The rectifier is designed to harvest RF energy at the frequency of 5.8 GHz. The Schottky diode SMS7630 has been chosen for this design because of its low turn-on voltage; the SPICE model parameters of this diode are shown in Table 1.

**TABLE 1.** SPICE model parameters of SMS7630 schottky diode.

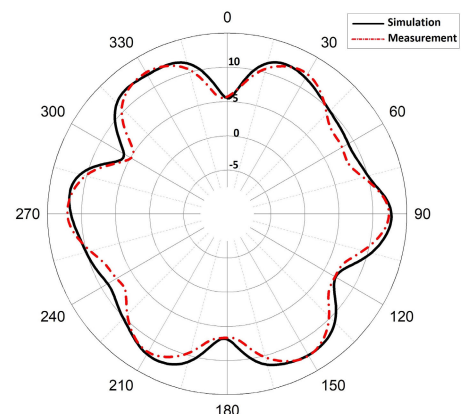| $Rs(\Omega)$ | 12 | $V_J (V)$ | 0.1 |
|---|---|---|---|
| N | 1.05 | M | 0.51 |
| TT (seg) | $10^{-11}$ | Eg (eV) | 0.35 |
| XTI | 2 | Fc | 0.69 |
| $B_V (V)$ | 3 | $I_{BV} (A)$ | 0.5 |
| $B_V (V)$ | 3 | $I_{BV} (A)$ | $10^{-5}$ |

The rectifier was fabricated using RT/Duroid 5880 substrate (dielectric constant is 2.2) with a dimension of $20 \times 15$ mm$^2$ and a thickness of 0.787 mm. The advanced system design 2019 (ADS) was used to optimize all the rectifier's parameters. To achieve accurate results, the nonlinear SPICE
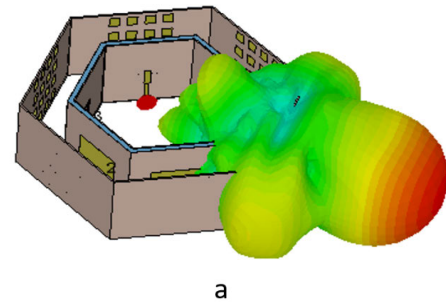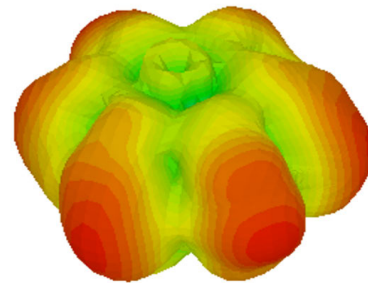


**FIGURE 13.** The 3D and polar radiation pattern of the proposed energy-harvesting antenna at resonance frequency 5.8 GHz: (a) one element; (b) six elements;(c) radiation pattern on the azimuth plane.

model of the diode and the S-parameters of the inductors and the capacitor provided by the manufacturer were considered in the simulation.

At a $-10$ dBm input power level, single-stub tuning (Lstub2) and an SMD inductor were employed to obtain satisfactory impedance matching. The low pass filter is a 100-pF capacitor that is used to pass only DC power to the load.

The choice of the output resistance (the load) is also very important and should be carefully made. For that purpose, a parametric study was conducted using ADS, illustrated in Figure 15. The conversion efficiency decreases with the increase in the value of the load. An efficiency of 44.5% is achieved for $R_L$ equals 3.65 K$\Omega$, and a 40% efficiency is achieved for a load of 7 K$\Omega$ for $-10$dBm.
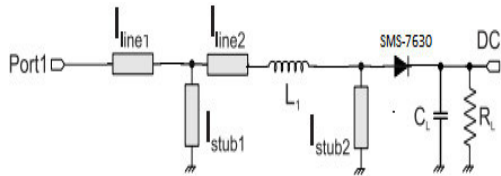
**FIGURE 14.** Schematic of the rectifier (Lline1 = 5 mm, Lline2 = 3 mm, Lstub1 = 4.5 mm, Lstub2 = 5.5 mm, L1 = 3.50 nH, and the width of the transmission lines is W = 2.38 mm, RL = 3.65 KΩ).

The performance of the proposed RF energy harvesting rectifier is measured in the lab, which is shown in Figure 16. The rectifier reflection coefficient was measured using The Rohde and Schwarz VNA. The signal generator was used to inject RF power to the rectifier, then we use a multi-meter to measure the output dc voltage to find the output dc power and RF-to-dc efficiency.
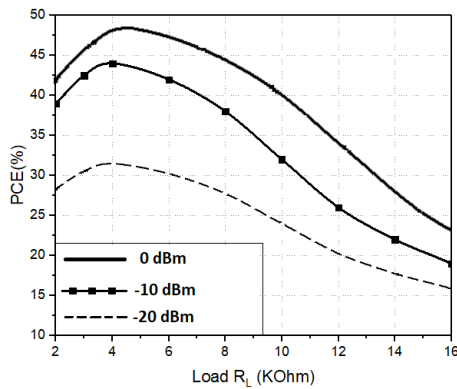


**FIGURE 15.** RF-to-DC conversion efficiency versus load versus different inputs power.
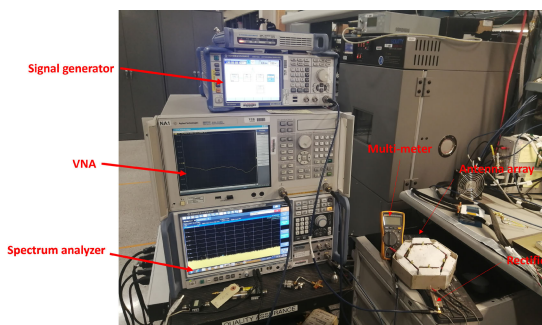


**FIGURE 16.** Rectifier measurement in the Lab.

Figure 17 shows the simulated and measured reflection coefficient of the rectifier at an input power level of −10 dBm. The rectifier performs well at 5.8 GHz with good impedance matching.

Figure 18 depicts the measured reflection coefficient of the rectifier versus the frequency at various input power levels. The rectifier works well at an input power level of −10 dBm. For input powers greater than −10 dBm, the reflection coefficient shifts toward high frequencies. For input powers below
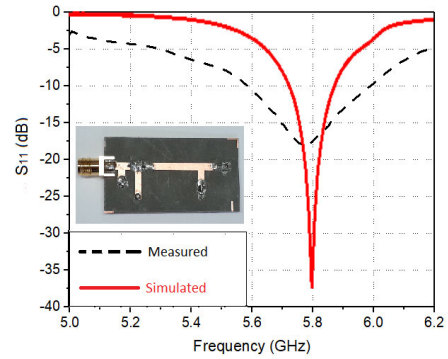


**FIGURE 17.** Simulated and measured reflection coefficient of the rectifier at −10 dBm.

−10 dBm, the reflection coefficient of the rectifier shifts toward low frequencies. For a power of −20 dBm, the reflection coefficient of the rectifier is equal to −8 dB at the frequency 5.8 GHz.

The RF-to-DC conversion efficiency of the rectifier various inputs power is depicted in Figure 19. For an input power level of −10 dBm, the measured results have led to a PCE of around 44.2% at the frequency 5.8 GHz with a peak of 48.5% at the 5.89 GHz frequency. It can be noticed that the peak appeared at the frequency 5.89 instead of 5.8 GHz is due to the shift introduced by the nonlinearity of the diode when operating at higher input power. However, for an input power of −20 dBm, a very low efficiency of 28% is obtained.
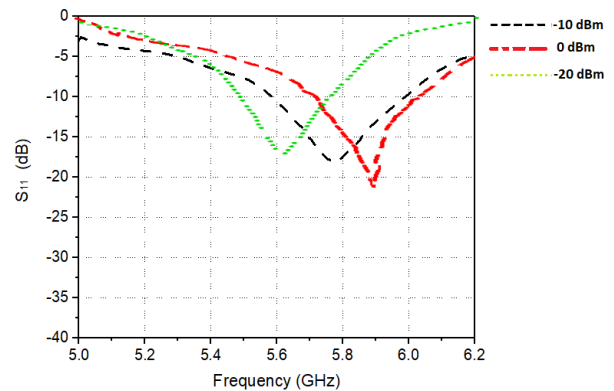


**FIGURE 18.** Measured reflection coefficient of the rectifier versus frequency at different input power levels.

The simulated and measured results of the output DC voltage as a function of the available input power at a frequency of 5.8 GHz are shown Figure 20. It can be seen that a good agreement is obtained between both results. Hence, for an input power of −10 dBm, a DC voltage of 0.423 V is obtained.

This rectifier has demonstrated good performance. As a result, a significant increase in output voltage can be achieved by utilizing a DC combiner to add the DC voltages from all six ports.
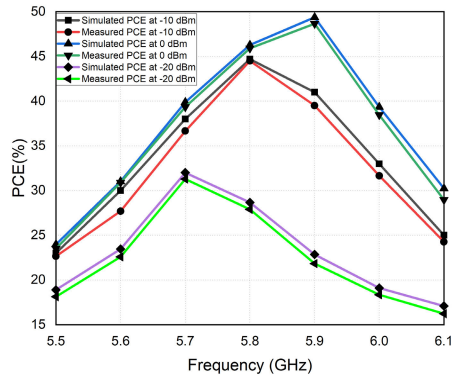
**FIGURE 19.** Simulated and Measured RF-to-DC conversion efficiency versus frequency at various input powers with a 3.65 K Ω load.
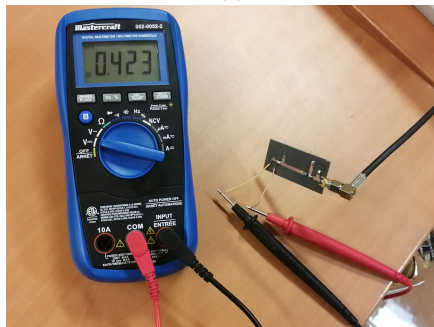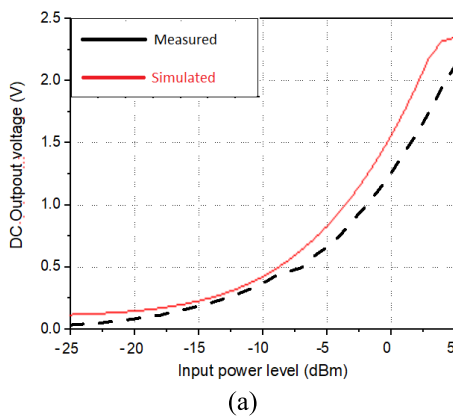


(a)



(b)

**FIGURE 20.** Measured output DC voltage (a) versus available input power at the frequency band of 5.8 GHz; (b) rectifier under test at −10 dBm.

## IV. RECTENNA EXPERIMENTAL TESTING

The measurement system of a proposed hexagonal rectenna is shown in Figure. 21. The Keysight RF signal generator is connected to the amplifier with an integrated attenuator that can be used to vary its gain from 0 dB to 32 dB. Afterward, the amplifier is connected to the antenna. The transmitting element is an omnidirectional antenna used in Distributed Antenna System (DAS) with a gain of 3 dB in the frequency range of 2–6 GHz. We chose the distance (D) between the transmitter and the receiver antenna so that the far-field condition applies to 5.8 GHz. To get a received power of −10 dBm, the initial distance was set at 1.5 m, and the PA gain was

increased to 17 dBm. The power received by the antenna is measured using Keysight spectrum analyzer. To change the antenna's power level, the distance D was changed by 0.5 m. The received power was measured at various distances as depicted on Figure 22. Table 2 shows also the antenna's received power as a function of distance.

Then in the position of a spectrum analyzer, one rectifier is connected to one port of the antenna array. Every other port is terminated by a 50 Ω load. The output voltage is measured with a multimeter at the same distances that the received power was measured. The RF conversion efficiency of the rectenna can be calculated using the corresponding output voltage, input power, and load resistance of 4 K. Figure 23 depicts the output DC power. The technique of DC combining is used in ambient RF energy harvesting, where each antenna port is connected to the rectifier and the output DC voltages or currents are added to the same load. In this case we used DC combining for the proposed hexagonal rectenna array. In fact, six rectifiers are fabricated and connected to each port of the array as illustrated in Figure 23.
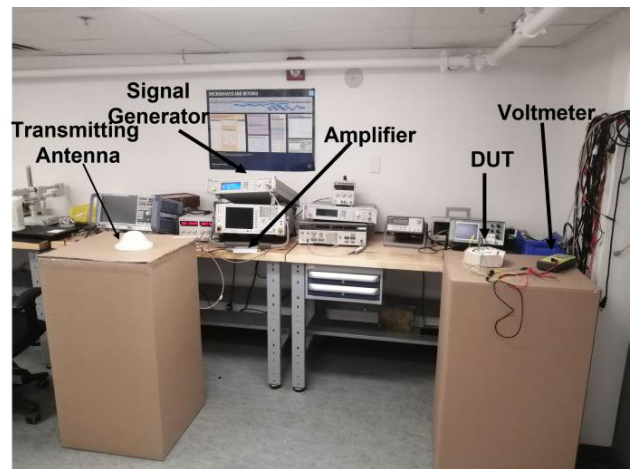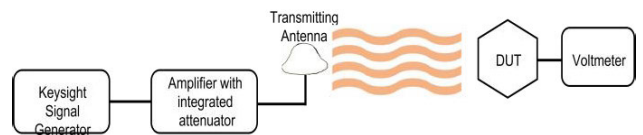


**FIGURE 21.** Test setup schematic and photograph of the proposed antenna with one rectifier.

**TABLE 2.** Received power at the antenna versus distance.

| Distance (m) | 1 | 1.5 | 2 | 2.5 | 3 | 3.5 |
|---|---|---|---|---|---|---|
| Received power (dBm) | −7 | −10 | −13 | −15 | −16.5 | −17.8 |

The second experiment is carried out with a similar procedure as the first one, but in this case, a DC combiner was used to combine the voltage from all the rectifiers.

**TABLE 3.** Comparison of the proposed antenna array with other works reported in the literature.

| Ref | Frequency (GHz) | Coverage in the azimuth plane (°) | Maximum gain (dBi) | Additional circuitry | Polarization | No of port | RF Input power Level (dBm) | Maximum RF TO DC Efficiency (%) |
|---|---|---|---|---|---|---|---|---|
| [9] | 2.4 | Full coverage | 4.62 | Butler matrix | Linear | 4 | -20 to 0 | 45 |
| [11] | 2.45 | (146°) | 5.9 | Butler matrix | Linear | 4 | -20 to 10 | 42 |
| [12] | 1.8–2.1 Broadband | (109°) | 4.25 | No | Linear | 1 | -20 t0 0 | 55 |
| [13] | 5.8 | Directional | 6.4 | No | Circular | 25 | -20 to 0 | 66.2 |
| [14] | 0.9, 1.8, 2.4 | Full coverage | 1.6, 2.4, 5.3 | No | Linear | 4 | -30 to 0 | 40 |
| [15] | 5.8 | (90°) | 4.7 | No | Linear | 1 | -20 to 10 | 61 |
| [16] | 5.8 | Directional | 15 | No | Linear | 1 | 0 to 10 | 52.55 |
| [17] | 2.45 | Full coverage | 6 | 3 × 3 network | Linear | 3 | -20 to 20 | 50 |
| [18] | 0.850, 1.81, 2.18, 2.40 | Not full | 3.95, 4.45, 4.42, 4.82 | no | Linear | 2 | -20 | 48 |
| [19] | 0.9, 1.8, 2.12, 2.4 | Not full | Not reported | no | Linear | 8 | -10 t0 -35 | 52 |
| This Work | 5.8 | Full coverage | 12.9 | No | Circular | 6 | -7 t0 -18 | 67.75 |
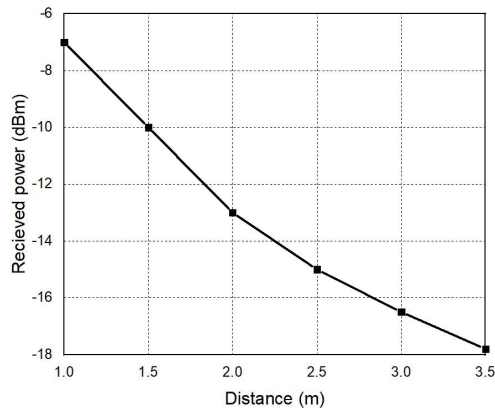


**FIGURE 22.** Received power at the antenna versus distance.



**FIGURE 24.** DC/PCE of the rectenna array versus the received power.

The conversion efficiency of the rectenna's array with respect to the received power at the antenna is plotted in Figure 24.
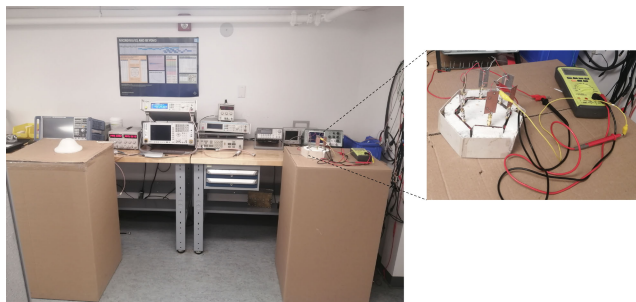


**FIGURE 23.** Test setup schematic and photograph of the proposed antenna with DC combiner.

According to Figure 24, The PCE of the rectenna array reaches 67.75 % at −10 dbm (1.5 m), in the other hand the PCE of the rectenna with one rectifier equals 41% at −10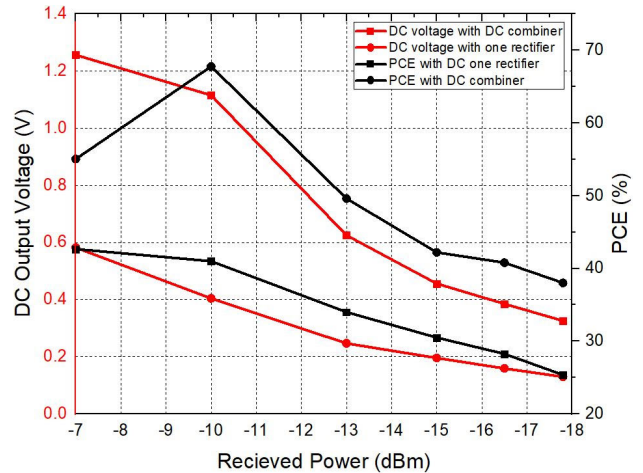 dBm (1.5 m), this value is a bit different from the PCE found before with the rectifier alone (44.5%). This discrepancy can be explained by the fact that in the harmonic balance simulation, the connector was not modelled very well, which changed the rectifier's input impedance and thus caused more reflection. The PCE gradually decreases with distance until it reaches a value of 25.36% at -17.8 dBm (3.5 m).

The DC voltage of the rectenna array with one rectifier and with the DC combiner is also plotted in Figure 24. With the DC combiner configuration, a DC voltage of 1.115 V is recorded at 1.5 m (−10 dBm), while a voltage of 0.404 is obtained in the case of a single rectifier, and this proves the capability of the antenna array to take advantage of the multi-path propagation by absorbing both line-of-sight propagation as well as reflected waves from all the angles in the azimuth plane. In addition, the rectenna array can absorb RF energy from both vertical and horizontal polarized waves given its CP characteristic.

A comparison between the proposed antenna array and other works is reported in Table 3. The hexagonal array

configuration shows better features in terms of the coverage and simplicity of fabrication compared to other techniques, in addition to that the circular polarization characteristic of the antenna allows more immunity to misalignment.

## V. CONCLUSION

This paper describes a novel high-gain CP hexagonal rectenna array for ambient RF energy harvesting. The proposed hexagonal array is composed of 6 antennas and 6 FSS layers to enhance the gain. The obtained results show that the proposed array can fully cover the entire azimuth plane with a high gain in all directions. The structure of the proposed array was low profile, easy to fabricate, and with no need to use any additional circuitry. It was demonstrated that the rectifier provides a good DC voltage as well as efficiency for a low-input RF power level of $-10$ dBm. The performance of the rectenna with one rectifier and six rectifiers using the DC combiner has been investigated. According to the results of the experiment, the output DC power of the DC combiner rectenna is about three times more than that of the single rectifier rectenna. The proposed hexagonal rectenna array design is a good candidate for WSNs.

## REFERENCES

[1] V. Kuhn, C. Lahuec, F. Seguin, and C. Person, "A multi-band stacked RF energy harvester with RF-to-DC efficiency up to 84%," *IEEE Trans. Microw. Theory Techn.*, vol. 63, no. 5, pp. 1768–1778, May 2015, doi: 10.1109/TMTT.2015.2416233.

[2] V. Palazzi, J. Hester, J. Bito, F. Alimenti, C. Kalialakis, A. Collado, P. Mezzanotte, A. Georgiadis, L. Roselli, and M. M. Tentzeris, "A novel ultra-lightweight multiband rectenna on paper for RF energy harvesting in the next generation LTE bands," *IEEE Trans. Microw. Theory Techn.*, vol. 66, no. 1, pp. 366–379, Jan. 2018, doi: 10.1109/TMTT.2017.2721399.

[3] M. Pinuela, P. D. Mitcheson, and S. Lucyszyn, "Ambient RF energy harvesting in urban and semi-urban environments," *IEEE Trans. Microw. Theory Techn.*, vol. 61, no. 7, pp. 2715–2726, Jul. 2013, doi: 10.1109/TMTT.2013.2262687.

[4] H. J. Visser, A. C. F. Reniers, and J. A. C. Theeuwes, "Ambient RF energy scavenging: GSM and WLAN power density measurements," in *Proc. 38th Eur. Microw. Conf.*, Oct. 2008, pp. 721–724, doi: 10.1109/EUMC.2008.4751554.

[5] M. Arrawatia, M. S. Baghini, and G. Kumar, "Differential microstrip antenna for RF energy harvesting," *IEEE Trans. Antennas Propag.*, vol. 63, no. 4, pp. 1581–1588, Apr. 2015, doi: 10.1109/TAP.2015.2399939.

[6] M. C. Derbal and M. Nedil, "A high gain rectenna for energy harvesting applications," in *Proc. IEEE Int. Symp. Antennas Propag. USNC-URSI Radio Sci. Meeting*, Jul. 2019, pp. 1505–1506, doi: 10.1109/APUSNCURSINRSM.2019.8888968.

[7] H. Sun and W. Geyi, "A new rectenna using beamwidth-enhanced antenna array for RF power harvesting applications," *IEEE Antennas Wireless Propag. Lett.*, vol. 16, pp. 1451–1454, Dec. 2016, doi: 10.1109/LAWP.2016.2642124.

[8] F. Xie, G.-M. Yang, and W. Geyi, "Optimal design of an antenna array for energy harvesting," *IEEE Antennas Wireless Propag. Lett.*, vol. 12, pp. 155–158, 2013, doi: 10.1109/LAWP.2013.2243697.

[9] E. Vandelle, D. Bui, T. Vuong, G. Ardila, K. Wu, and S. Hemour, "Harvesting ambient RF energy efficiently with optimal angular coverage," *IEEE Trans. Antennas Propag.*, vol. 67, no. 3, pp. 1862–1873, Mar. 2019, doi: 10.1109/TAP.2018.2888957.

[10] K. Niotaki, S. Kim, S. Jeong, A. Collado, A. Georgiadis, and M. M. Tentzeris, "A compact dual-band rectenna using slot-loaded dual band folded dipole antenna," *IEEE Antennas Wireless Propag. Lett.*, vol. 12, pp. 1634–1637, 2013, doi: 10.1109/LAWP.2013.2294200.

[11] D.-J. Lee, S.-J. Lee, I.-J. Hwang, W.-S. Lee, and J.-W. Yu, "Hybrid power combining rectenna array for wide incident angle coverage in RF energy transfer," *IEEE Trans. Microw. Theory Techn.*, vol. 65, no. 9, pp. 3409–3418, Sep. 2017, doi: 10.1109/TMTT.2017.2678498.

[12] C. Song, Y. Huang, J. Zhou, J. Zhang, S. Yuan, and P. Carter, "A high-efficiency broadband rectenna for ambient wireless energy harvesting," *IEEE Trans. Antennas Propag.*, vol. 63, no. 8, pp. 3486–3495, Aug. 2015, doi: 10.1109/TAP.2015.2431719.

[13] Y. Yang, J. Li, L. Li, Y. Liu, B. Zhang, H. Zhu, and K. Huang, "A 5.8 GHz circularly polarized rectenna with harmonic suppression and rectenna array for wireless power transfer," *IEEE Antennas Wireless Propag. Lett.*, vol. 17, no. 7, pp. 1276–1280, Jul. 2018, doi: 10.1109/LAWP.2018.2842105.

[14] F. Khalid, W. Saeed, N. Shoaib, M. U. Khan, and H. M. Cheema, "Quad-band 3D rectenna array for ambient RF energy harvesting," *Int. J. Antennas Propag.*, vol. 2020, pp. 1–23, May 2020, doi: 10.1155/2020/7169846.

[15] X. Cai, W. Geyi, and Y. Guo, "A compact rectenna with flat-top angular coverage for RF energy harvesting," *IEEE Antennas Wireless Propag. Lett.*, vol. 20, no. 7, pp. 1307–1311, Jul. 2021, doi: 10.1109/LAWP.2021.3078548.

[16] U. Pattapu and S. Das, "Capacitive coupled circular patch antenna based rectenna systems for 5.8 GHz wireless power transfer applications," *Int. J. RF Microw. Comput.-Aided Eng.*, vol. 31, no. 7, pp. 1–10, Apr. 2021, doi: 10.1002/mmce.22675.

[17] H. Sun, J. Huang, and Y. Wang, "An omnidirectional rectenna array with an enhanced RF power distributing strategy for RF energy harvesting," *IEEE Trans. Antennas Propag.*, vol. 70, no. 6, pp. 4931–4936, Jun. 2022, doi: 10.1109/TAP.2021.3138542.

[18] S. Roy, J. J. Tiang, M. B. Roslee, M. T. Ahmed, A. Z. Kouzani, and M. A. P. Mahmud, "Quad-band rectenna for ambient radio frequency (RF) energy harvesting," *Sensors*, vol. 21, no. 23, p. 7838, Nov. 2021, doi: 10.3390/s21237838.

[19] S. Roy, J.-J. Tiang, M. B. Roslee, M. T. Ahmed, A. Z. Kouzani, and M. A. P. Mahmud, "Design of a highly efficient wideband multi-frequency ambient RF energy harvester," *Sensors*, vol. 22, no. 2, p. 424, Jan. 2022, doi: 10.3390/s22020424.

**MOHAMMED CHERIF DERBAL** was born in Chelghoum Laïd, Algeria. He received the State Engineering degree in electronics from Ecole Nationale Polytechnique, Algiers, in 2017, and the master's degree from the University of Quebec, Quebec, Canada, in 2019. His research interests include RF energy harvesting, optimization algorithms, MIMO antennas and radio-wave propagation, and microwave devices.

**MOURAD NEDIL** (Senior Member, IEEE) received the Dipl.-Ing. degree from the University of Science and Technology Houari Boumediene, Algiers, Algeria, in 1996, the D.E.A. (M.S.) degree from the University of Paris-Est Marne-la-Vallée, Marne la Vallée, France, in 2000, and the Ph.D. degree from the Institut National de la Recherche Scientifique (INRS-EMT), Université de Québec à Montréal, Montréal, QC, Canada, in April 2006. He received the Postdoctoral Fellowship from INRS-EMT, within the RF Communications Systems Group, in 2008. In June 2008, he joined the Engineering School, University of Quebec at Abitibi-Témiscamingue, Canada, where he is currently a Full Professor. His research interests include antennas, MIMO radio-wave propagation, and microwave devices.

• • •